TEMPO-Oxidized Cellulose Nanofiber Hydrogel Electrolyte for Rechargeable Zn-Ion Battery

Kento Kimura[ab], Vittorio Marangon[cd], Taiga Fukuda[e], Mana Suzuki[e], Nantapat Soontornnon[e],

Yoichi Tominaga*[abe], Jusef Hassoun*[bcd]

[a] *Department of Applied Chemistry, Graduate School of Engineering, Tokyo University of Agriculture and Technology, 2-24-16, Naka-cho, Koganei-shi, Tokyo 184-8588, Japan.*

[b] *Institute of Global Innovation Research (GIR), Tokyo University of Agriculture and Technology, 2-24-16, Naka-cho, Koganei-shi, Tokyo 184-8588, Japan.*

[c] *Department of Chemical, Pharmaceutical and Agricultural Sciences, University of Ferrara, Via Fossato di Mortara 17, 44121, Ferrara, Italy.*

[d] *Graphene Labs, Istituto Italiano di Tecnologia, Via Morego 30, Genoa 16163, Italy*

[e] *Graduate School of Bio-Applications and Systems Engineering (BASE), Tokyo University of Agriculture and Technology, 2-24-16, Naka-cho, Koganei-shi, Tokyo 184-8588, Japan.*

*Corresponding Author: jusef.hassoun@unife.it (J. Hassoun); ytominag@cc.tuat.ac.jp (Y. Tominaga)

Keywords

Supplementary Information

Contains 8 Figures and 1 Table.

A hydrogel benefiting of 2,2,6,6-tetramethyl-1-piperidinyloxy (TEMPO)-oxidized cellulose nanofiber (TOCNF) in low concentration, $Zn(ClO_4)_2$ conducting salt and water as main matrix was evaluated as an electrolyte for rechargeable zinc batteries in the Manuscript. Rheological measurements showed strong shear-thinning behavior and thixotropic properties of the TOCNF-based hydrogel electrolyte in the static state, while the evaluation of ionic conductivity, compatibility with zinc metal anode via EIS, and Zn plating/stripping and electrochemical stability window suggested suitable properties for application in rechargeable zinc batteries. The CV test revealed that the initial discharge of the $Zn|MnO_2$ cell using the TOCNF-based hydrogel electrolyte evolves at 1.0 V vs. Zn^{2+}/Zn through reduction of β-MnO_2 to MnOOH and dissolved Mn^{2+}, with insertion of H^+ and Zn^{2+} ions into the electrode framework. The test also indicated that the subsequent charge occurs between 1.5 and 1.6 V vs. Zn^{2+}/Zn, with complex oxidation of MnOOH and Mn^{2+} to ε-MnO_2 and extraction of H^+. The subsequent cycles revealed that the cell progressively undergoes a well reversible redox process centered at 1.5 V vs. Zn^{2+}/Zn with decreasing charge/discharge polarization, increasing intensity, and resistance shrinking from 140 Ω to below 20 Ω. The electrolyte demonstrated in a $Zn|MnO_2$ cell a reversible behavior evolving from 1.5 to 1.0 V, with a maximum capacity of 110 mAh g^{-1} after the initial cycle, which is retained for over 60% upon 50 charge/discharge cycles. This promising performance suggests the TOCNF-based hydrogel electrolyte as possible candidate to obtain environmentally sustainable *solid-like* rechargeable zinc-ion battery, despite optimizations of

materials and testing conditions are certainly required to increase the cell cycle life. In this regard, a self-healable hydrogel electrolyte was reported in literature for quasi-solid-state $Zn-MnO_2$ battery, where the electrolyte was formed by carboxyl-modified poly(vinyl alcohol) cross-linked by COO–Fe bonding in the presence of $Zn(NO_3)_2$ and $MnSO_4$. That battery delivered a specific capacity up to 177 mAh g^{-1} retained for 83% over long cycling (see ref 33 in the Manuscript). Another report showed a hydrogen bond acceptor lined hydrogel having three-dimensional network with dimethyl sulfoxide (DMSO), H_2O and polymer chains, which was used in $Zn//MnO_2$ battery with a capacity of 238 mAh g^{-1} over long cycling (see 34 in the Manuscript). In addition, a self-adapting and self-healing hydrogel was prepared by in-situ cross-linking reaction with long cycling stability in Zn/MnO_2 cell and a delivered capacity ranging from 200 to 250 mAh g^{-1} (see ref 35 in the Manuscript). Despite all these cells exceed in capacity and cycling stability the cell reported in our Manuscript, we would mention that our $Zn|MnO_2$ cell exploits for the first time the TEMPO-oxidized CNF hydrogel in Zn rechargeable battery which is a simple and suitable approach for achieving this challenging battery.

Experimental

Samples preparation. TOCNF-based hydrogel containing 2 wt.% TOCNF with respect to water (Rheocrysta I-2SX) was provided by DKS Co. Ltd. and used as received. The diameter and length of the CNFs were of 3 nm and 800–1000 nm, respectively, and the material was rearranged into microfibrils, i.e., the basic building blocks formed by the crystallization of cellulose molecules. Zinc perchlorate hexahydrate ($Zn(ClO_4)_2·6H_2O$, FUJIFILM Wako Pure Chemical and Sigma-Aldrich) was

used as received as conducting salt. The hydrogel electrolyte was prepared by adding 3.15 g of

$Zn(ClO_4)_2 \cdot 6H_2O$ to 5 g of the TOCNF-based hydrogel to achieve a concentration close to 3mol% of

conducting salt with respect to water, followed by 1 hour of mixing via a magnetic stirrer. As a

reference sample, a salt-free hydrogel with the same TOCNF content with respect to water was

prepared by adding 0.91 g of deionized water, which is equivalent to the hydration water in the 3.15 g

of $Zn(ClO_4)_2 \cdot 6H_2O$, to 5 g of the TOCNF-based hydrogel, followed by 1 hour of stirring. The

concentration of TOCNF and $Zn(ClO_4)_2$ in the hydrogels are summarized in Table S1.

Table S1. Composition of the hydrogel samples.

Sample	TOCNF : H_2O weight ratio	$Zn(ClO_4)_2$: H_2O molar ratio
TOCNF reference hydrogel	1.7 : 98.3	N/A
TOCNF hydrogel electrolyte	1.7 : 98.3	2.62 : 100.00

Electrode preparation. A composite MnO_2-based cathode for charge/discharge test was prepared by

mixing pyrolusite manganese dioxide powder (β-MnO$_2$, >99%, Sigma-Aldrich) as active material,

carbon black (CB, Super P, TIMCAL) as conducting additive and poly(vinylidene fluoride) (PVdF,

Solef 6020, Solvay) as binder in the 80:10:10 weight ratio with N-methyl-2-pyrrolidone (NMP, Sigma-

Aldrich) as dispersing solvent. The resulting slurry was applied onto a graphite foil (thickness of 120

μm, Mathis AG) using a doctor blade tool (film thickness of 350 μm, MTI corp.) and dried at 60 °C

for 3 h. The electrode tape was then punched into disks with diameter of 10 mm. The final MnO_2 areal

loading was ~1.3 mg cm^{-2}.

Characterization. The pH values of the TOCNF-based hydrogel without salt and of the electrolyte were measured by using a pH-meter (AS ONE). Fourier-transform infrared spectroscopy (FT-IR) was conducted using the FT-IR-4100 (Jasco Co.) equipped with an ATR unit (ZnSe lens) in the wavenumber range from 700 to 4000 cm^{-1} at a resolution of 4 cm^{-1}, with a total of 96 scans. Rheological measurements were carried out for the hydrogel electrolyte and the salt-free hydrogel using an HR-30 stress-controlled rheometer (TA Instruments) equipped with an aluminum parallel plate with a diameter of 40 mm by setting the measuring gap at 500 μm. Flow curves were acquired by increasing the shear rate logarithmically from 0.001 to 1000 s^{-1} over 3 min and then decreasing it to 0.001 s^{-1} over 3 min. Strain sweep of dynamic viscoelasticity measurement was conducted from 0.01% to 1000% at an angular frequency of 6.28 rad s^{-1}. Frequency sweep was then performed with the strain of linear viscoelastic region, i.e., 0.1% in this study, by decreasing the angular frequency from 100 to 0.1 rad s^{-1}. These dynamic viscoelasticity tests were initiated after 3 min rest periods. The temperature for all the measurements was controlled at 25 °C by a Peltier plate. X-ray photoelectron spectroscopy (XPS) was performed using a JPS-9030 photoelectron spectrometer (JEOL Ltd.) equipped with a Mg-Kα source operating at 10 kV to assess the chemical bonding environment of the substances on Zn anode surface. Pristine Zn in contact with atmosphere (i.e., H_2O, O_2, N_2, CO_2) was directly analyzed, while for the Zn metal after aging in contact with the hydrogel electrolyte the surface was rinsed with deionized water and subsequently dried at 100 °C in a glass tube under reduced pressure for 1 h prior to measurement. The electrochemical characterization of the hydrogel electrolyte

was performed using a T-type Swagelok polyethylene cell, with stainless-steel (SS) electrodes having a diameter of 10 mm suitable both for two- or three-electrode configurations. The ionic conductivity at 25 °C was measured by electrochemical impedance spectroscopy (EIS) on symmetric two-electrode cells with blocking setup, where the hydrogel was held between the two SS-cylinders by a polytetrafluoroethylene (PTFE) O-ring with thickness of 800 µm, external diameter of 10 mm and internal one of 6 mm, to fix the cell constant at 0.283 cm^{-1}. EIS was conducted in a frequency range from 1 kHz to 100 Hz with a voltage amplitude of 10 mV. The compatibility of the electrolyte with zinc metal (foil thickness of 80 µm, Metalnastri) was evaluated by performing EIS measurements every day for 6 days on a symmetric Zn|Zn cell using the two-electrode configuration and the above PTFE O-ring. A frequency range from 500 kHz to 0.02 Hz was employed for the EIS tests alongside a voltage amplitude of 10 mV. A galvanostatic plating/stripping test was performed on the same cell configuration at a current density of 0.2 mA cm^{-2} with a step time of 1 h for each charge and discharge. The subsequent investigations in cell were performed using a porous nylon fiber cloth with diameter of 10 mm as additional backbone (800 µm-thick, 50 PS/L, New Jet). Further tests with a membrane 300 µm-thick were performed for comparison. The full *in-situ* impregnation and diffusion of the gel into the nylon cloth was achieved by: *i)* pressing the hydrogel on both sides of the membrane; *ii)* heating at 45 °C for 3 h; *iii)* natural cooling to the room temperature (25 °C) for 3 h; *iv)* additional heating at 60 °C for 1 h, and *iv)* final cooling to 25 °C. The electrochemical stability window of the hydrogel electrolyte was determined using three-electrode configuration cell with a 10 mm-diameter

graphite disk as working electrode and a 10 mm-diameter zinc disk as the counter electrode, separated by two 10-mm gelled electrolyte membranes 800 μm-thick, and an additional zinc stripe as the reference electrode in between them. Linear sweep voltammetry (LSV) for anodic and cathodic regions was carried out from the open circuit voltage (OCV) condition of the cells to either 0.01 V vs. Zn/Zn^{2+} or to 2.20 V vs. Zn/Zn^{2+}, respectively, at a rate of 0.1 mV s^{-1}. Cycling voltammetry (CV) was performed on three-electrode configuration cell using a 10 mm-diameter MnO_2 disk as the working electrode and a 10 mm-diameter zinc disk as the counter electrode, separated by two 10-mm gelled electrolyte membranes 800 μm-thick, and additional Zn stripe as the reference electrode in between them. The CV was performed within the $0.8 - 1.7$ V vs. Zn^{2+}/Zn potential range at a scan rate of 0.1 mV s^{-1}. EIS tests were performed on the same cell at the OCV condition, and after 5 and 10 CV cycles within a frequency range from 500 kHz to 0.02 Hz exploiting a voltage amplitude of 10 mV. All EIS data were analyzed through non-linear least squares (NLLS) fitting method to evaluate the resistance values. The fitting was performed via the Boukamp software by associating the obtained Nyquist plots to equivalent circuits composed of resistive (R) and constant phase (Q) elements. Only fits with a χ^2 value of the order of 10^{-4} or lower were considered acceptable. Galvanostatic charge/discharge tests were performed in a two-electrode Zn|MnO_2 cell using only one 10-mm gelled electrolyte membrane either 800 or 300-μm thick, in the $0.8 - 1.7$ V voltage range at a C-rate of C/20 (1C = 308 mA g^{-1} as referred to the MnO_2 mass). Voltammetry and EIS were run through a VersaSTAT MC Princeton Applied Research (PAR-AMETEK) instrument, while the galvanostatic tests were performed via a

MACCOR Series 4000 battery test system. All the electrochemical measurements were carried out at

25 °C.

The room temperature conductivity of a $Zn(ClO_4)_2$ control aqueous solution for comparison with the TOCNF-based hydrogel electrolyte is determined to be of 1.8×10^{-1} S cm^{-1} from the Nyquist plot of Figure S1. See discussion of Figure 1 in the Manuscript for further details.
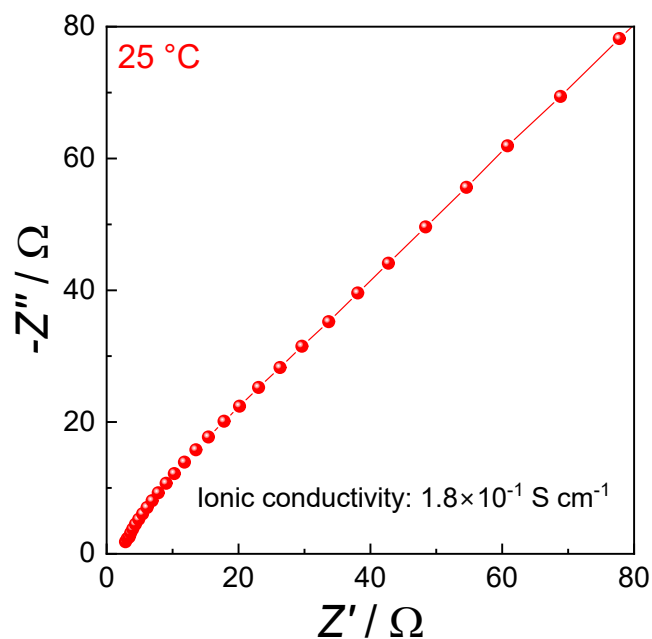
Figure S1. Nyquist plot related with the ionic conductivity measurement of a $Zn(ClO_4)_2$ 1M control aqueous solution at 25 °C; frequency range: 1 kHz – 100 Hz; voltage signal: 10 mV.

Figure S2 reports the flow curves for the TOCNF-based hydrogel with and without the $Zn(ClO_4)_2$ salt, and the corresponding measurement step under increasing shear rate (curves under decreasing shear rate are also reported in Figure 1b). The similar shape of the curves indicates marginal effect of the salt addition on the stability of the hydrogel. See Figure 1 in the Manuscript for further discussion.
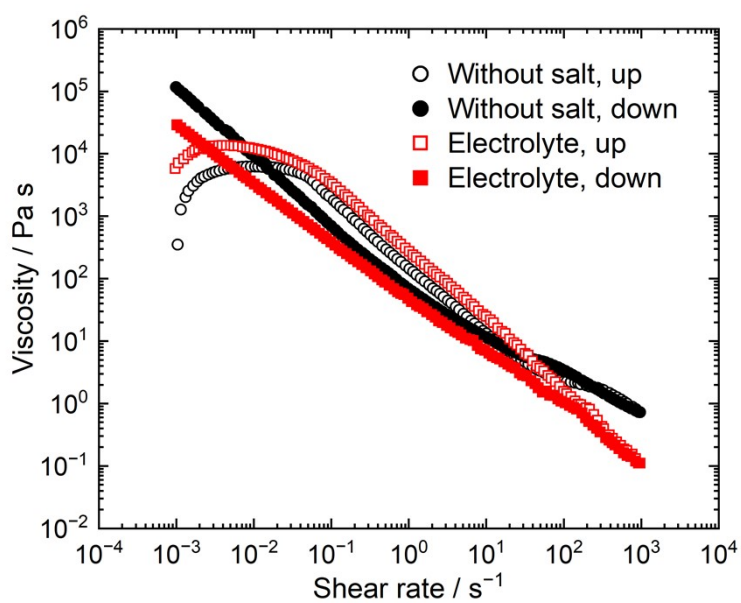
Figure S2. Flow curves of the TOCNF-based hydrogel without salt and the hydrogel electrolyte measured with increasing and decreasing shear rates at 25 °C.

Figure S3 shows the strain sweep curves of the TOCNF hydrogel with and without the $Zn(ClO_4)_2$ conducting salt, and shows for the salt-free hydrogel a dilatancy behavior, which is suppressed in the hydrogel electrolyte. See Figure 1 in the Manuscript for further discussion.
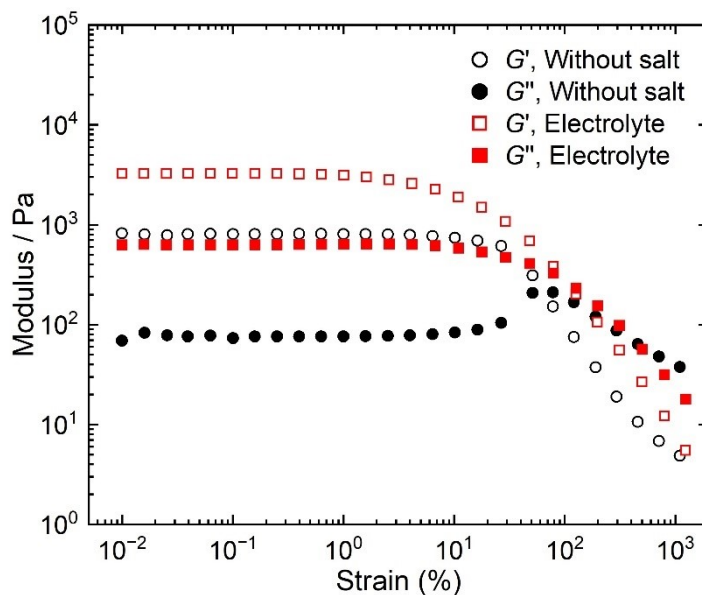
Figure S3. Strain dependences of storage modulus (G') and loss modulus (G'') of the TOCNF hydrogel without salt and the hydrogel electrolyte at 25 °C.

Figure S4 reports the voltage profiles (Figure S4a) and the cycling trend (Figure S4b) of a $Zn|MnO_2$ cell using a control aqueous solution of $Zn(ClO_4)_2$ (1 M), galvanostatically cycled at C/20 constant rate (1C = 308 mA g^{-1}) between 0.8 and 1.7 V at 25 °C. The cell displays a steady state capacity below 100 mAh g^{-1}, and a final capacity of 49 mAh g^{-1} upon 60 cycles, that is, a lower value compared to the TOCNF-based hydrogel electrolyte. See Figure 4 in the Manuscript for further discussion.
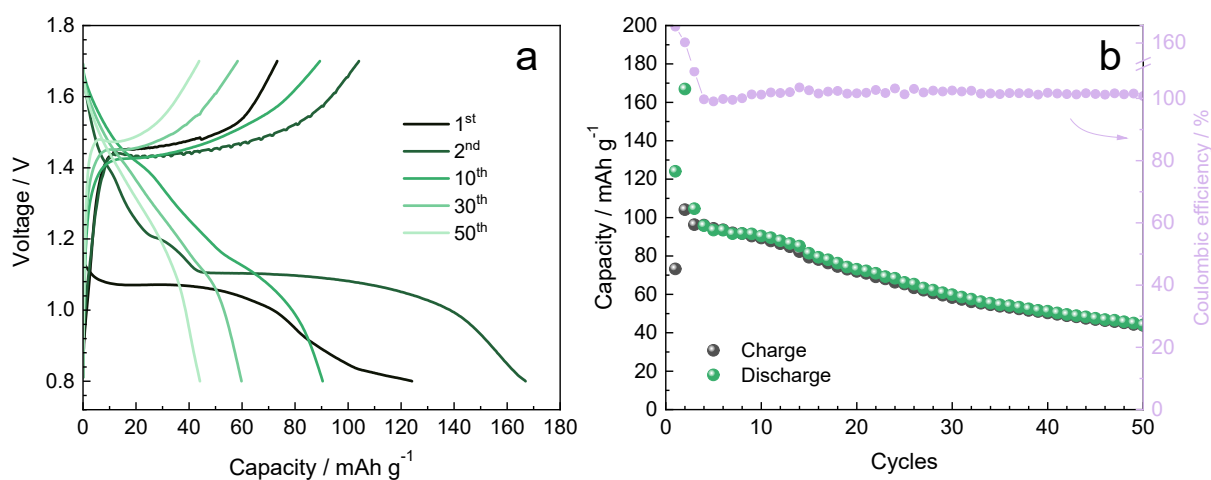
Figure S4. **(a)** Selected voltage profiles and **(b)** corresponding capacity trend with coulombic efficiency related to a galvanostatic charge/discharge cycling test of a $Zn|MnO_2$ cell using a control aqueous solution of $Zn(ClO_4)_2$ (1 M), performed at C/20 constant rate (1C = 308 mA g^{-1}) between 0.8 and 1.7 V at 25 °C.

The effect of the membrane thickness on cell performances is subsequently investigated. The results depicted in Figure S5 indicate a higher initial capacity when a thinner electrolyte membrane is used, that is, 180 mAh g^{-1} for an electrolyte 300 μm-thick instead of 165 mAh g^{-1} for the 800 μm-thick one. However, the figure also shows that the decrease of the thickness limits the stability due to possible cell configuration or geometry issues that should be still improved.
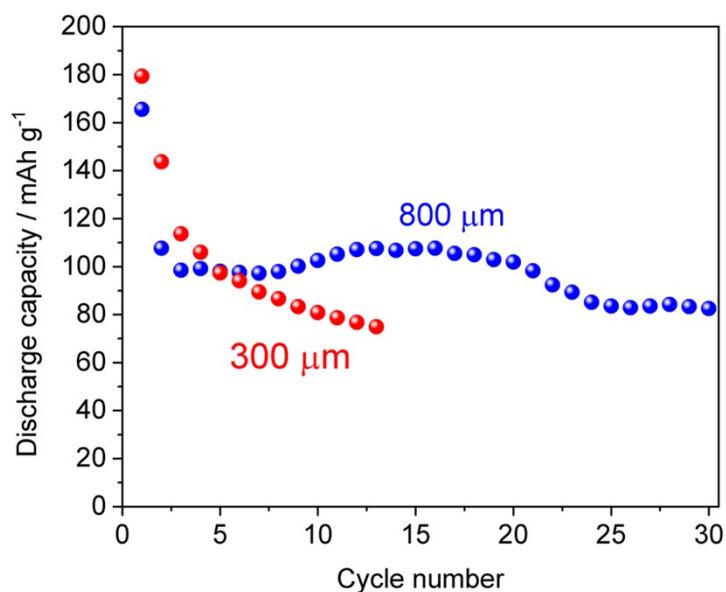
Figure S5. Galvanostatic cycling discharge capacity trends of Zn|MnO$_2$ cells using the TOCNF hydrogel electrolyte with thickness of 300 μm (red) and 800 μm (blue) performed at C/20 rate (1C = 308 mA g^{-1}) between 0.8 and 1.7 V at 25 °C.

Figure S6 reports a set of photographic images of the TOCNF hydrogel electrolyte, which appears as a semi-transparent gel.
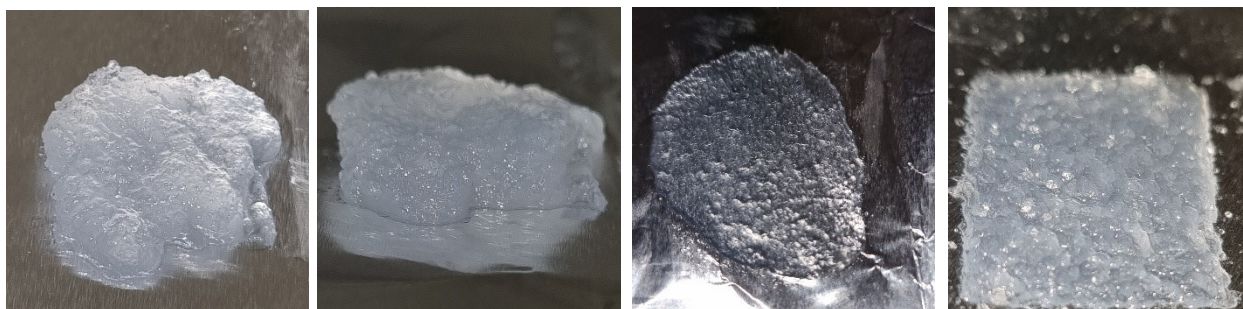
Figure S6. Set of photographic images of the TOCNF hydrogel electrolyte

Figure S7 depicts a schematic illustration of the structure of the TOCNF hydrogel electrolyte, and the expected reciprocal interactions between its components. The TOCNF should form a 3D network structure due to its high aspect ratio, which strengthens the stability of the gelled system. Additionally, the TOCNF has dense -COO$^-$ ionic functional groups originating from the TEMPO oxidation reaction. These anionic groups can form a coordination structure with Zn cations, which leads to a firm physical crosslinking effect to further strengthen the stability. These physical network and crosslinking structures enable the interesting shear-thinning and reversible mechanical transition (thixotropy) behaviors of the hydrogel electrolyte.
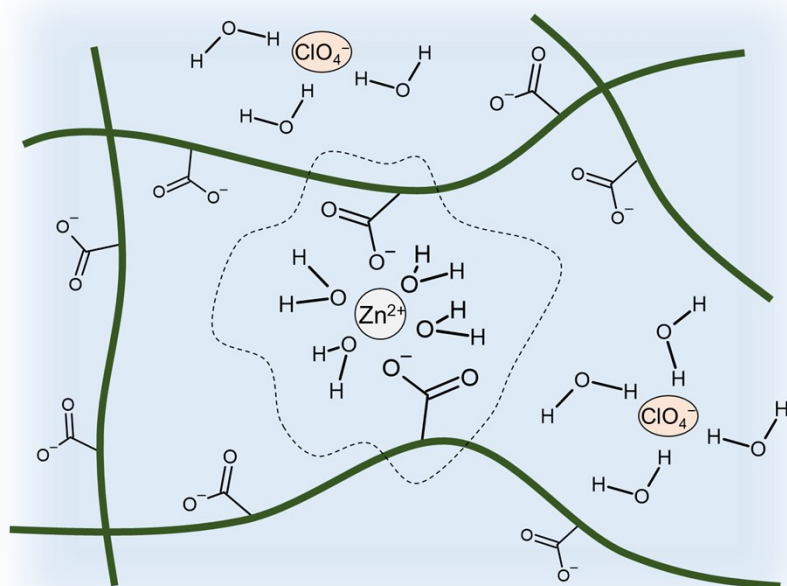
Figure S7. Schematic illustration of the expected internal interaction structures in the TOCNF hydrogel electrolyte.

Figure S8 illustrates the $Zn|MnO_2$ cells using TOCNF hydrogel electrolyte either with $ZnSO_4$ or

$Zn(ClO_4)_2$ salts. The data indicate that the change of the salt actually improves the capacity to a

maximum value of 140 mAh g^{-1} rather than 110 mAh g^{-1} and to a steady state of 110 mAh g^{-1} rather

than 80 mAh g^{-1}, respectively. Furthermore, the cycling test shows that the use of a different salt

improves the long term cycling, extending the battery life to 100 cycles. Therefore, these results

suggest a wide room for improvement of the battery performances both in terms of delivered capacity

and of stability by tuning carefully the cell chemistry and setup.
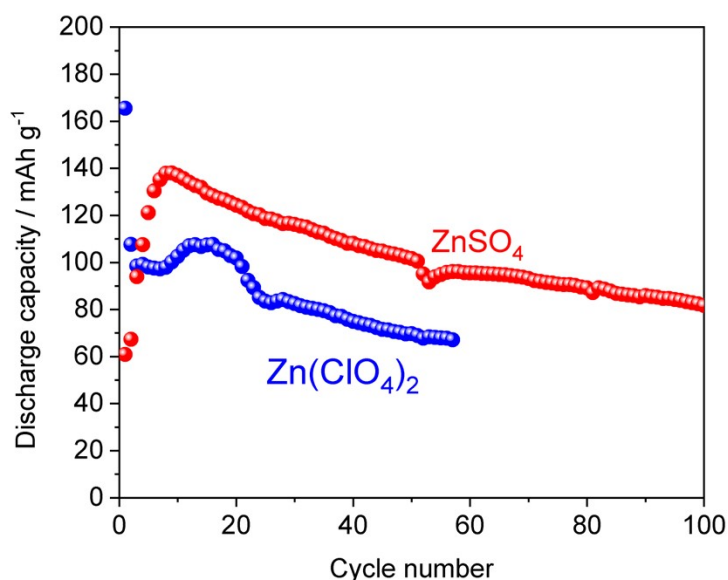
Figure S8. Galvanostatic cycling discharge capacity trends of $Zn|MnO_2$ cells using the TOCNF

hydrogel electrolyte either with $ZnSO_4$ salt (red) or $Zn(ClO_4)_2$ salt (blue), performed at C/20 rate (1C

= 308 mA g^{-1}) between 0.8 and 1.7 V at 25 °C.